Chip-based silica microspheres for cavity optomechanics

Xuefeng Jiang,[1,*] Min Wang,[1,2] Mark C. Kuzyk,[1] Thein Oo,[1] Gui-Lu Long,[2] and Hailin Wang[1]

[1]*Department of Physics and Oregon Center for Optics, University of Oregon, Eugene, Oregon 97403, USA*
[2]*State Key Laboratory of Low-dimensional Quantum Physics and Department of Physics, Tsinghua University, Beijing 100084, China*
[*]*xfjiang@uoregon.edu*

Abstract: We have experimentally realized on-chip silica microspheres that feature excellent thermal coupling to the silicon wafer. The chip-based microspheres significantly reduce laser-induced heating and correspondingly exhibit much lower threshold optical power for heating-induced optical bistability. We also show that the chip-based microspheres have optical and especially optomechanical properties that are similar to those of traditional fiber-stem-attached silica microspheres, making the chip-based microspheres suitable for optomechanical studies in a vacuum environment.

OCIS codes: (120.4880) Optomechanics; (120.6810) Thermal effects; (140.3945) Microcavities.

References and links

1. K. J. Vahala, "Optical microcavities," Nature **424**(6950), 839–846 (2003).
2. F. Vollmer and S. Arnold, "Whispering-gallery-mode biosensing: label-free detection down to single molecules," Nat. Methods **5**(7), 591–596 (2008).
3. J. Zhu, S. K. Ozdemir, Y. F. Xiao, L. Li, L. He, D. R. Chen, and L. Yang, "On-chip single nanoparticle detection and sizing by mode splitting in an ultrahigh-Q microresonator," Nat. Photonics **4**(1), 46–49 (2010).
4. L. Shao, X.-F. Jiang, X.-C. Yu, B.-B. Li, W. R. Clements, F. Vollmer, W. Wang, Y.-F. Xiao, and Q. Gong, "Detection of single nanoparticles and lentiviruses using microcavity resonance broadening," Adv. Mater. **25**(39), 5616–5620 (2013).
5. L. Yang, D. K. Armani, and K. J. Vahala, "Fiber-coupled erbium microlasers on a chip," Appl. Phys. Lett. **83**(5), 825–826 (2003).
6. X.-F. Jiang, Y.-F. Xiao, C.-L. Zou, L. He, C.-H. Dong, B.-B. Li, Y. Li, F.-W. Sun, L. Yang, and Q. Gong, "Highly unidirectional emission and ultralow-threshold lasing from on-chip ultrahigh-Q microcavities," Adv. Mater. **24**(35), OP260–OP264 (2012).
7. S. M. Spillane, T. J. Kippenberg, K. J. Vahala, K. W. Goh, E. Wilcut, and H. J. Kimble, "Ultrahigh-Q toroidal microresonators for cavity quantum electrodynamics," Phys. Rev. A **71**(1), 013817 (2005).
8. Y.-S. Park, A. K. Cook, and H. Wang, "Cavity QED with diamond nanocrystals and silica microspheres," Nano Lett. **6**(9), 2075–2079 (2006).
9. Y.-C. Liu, Y.-F. Xiao, B.-B. Li, X.-F. Jiang, Y. Li, and Q. Gong, "Coupling of a single diamond nanocrystal to a whispering-gallery microcavity: Photon transport benefitting from Rayleigh scattering," Phys. Rev. A **84**(1), 011805 (2011).
10. M. Aspelmeyer, T. J. Kippenberg, and F. Marquardt, "Cavity optomechanics," Rev. Mod. Phys. **86**(4), 1391–1452 (2014).
11. T. Carmon, H. Rokhsari, L. Yang, T. J. Kippenberg, and K. J. Vahala, "Temporal behavior of radiation-pressure-induced vibrations of an optical microcavity phonon mode," Phys. Rev. Lett. **94**(22), 223902 (2005).
12. T. J. Kippenberg, H. Rokhsari, T. Carmon, A. Scherer, and K. J. Vahala, "Analysis of radiation-pressure induced mechanical oscillation of an optical microcavity," Phys. Rev. Lett. **95**(3), 033901 (2005).
13. R. Ma, A. Schliesser, P. Del'haye, A. Dabirian, G. Anetsberger, and T. J. Kippenberg, "Radiation-pressure-driven vibrational modes in ultrahigh-Q silica microspheres," Opt. Lett. **32**(15), 2200–2202 (2007).
14. E. Verhagen, S. Deléglise, S. Weis, A. Schliesser, and T. J. Kippenberg, "Quantum-coherent coupling of a mechanical oscillator to an optical cavity mode," Nature **482**(7383), 63–67 (2012).
15. V. Fiore, Y. Yang, M. C. Kuzyk, R. Barbour, L. Tian, and H. Wang, "Storing optical information as a mechanical excitation in a silica optomechanical resonator," Phys. Rev. Lett. **107**(13), 133601 (2011).
16. V. Fiore, C. Dong, M. C. Kuzyk, and H. Wang, "Optomechanical light storage in a silica microresonator," Phys. Rev. A **87**(2), 023812 (2013).

#246334 Received 20 Jul 2015; revised 7 Sep 2015; accepted 8 Sep 2015; published 8 Oct 2015

17. C. Dong, V. Fiore, M. C. Kuzyk, and H. Wang, "Optomechanical dark mode," Science **338**(6114), 1609–1613 (2012).
18. C. Dong, V. Fiore, M. C. Kuzyk, and H. Wang, "Transient optomechanically induced transparency in a silica microsphere," Phys. Rev. A **87**(5), 055802 (2013).
19. G. Anetsberger, O. Arcizet, Q. P. Unterreithmeier, R. Rivière, A. Schliesser, E. M. Weig, J. P. Kotthaus, and T. J. Kippenberg, "Near-field cavity optomechanics with nanomechanical oscillators," Nat. Phys. **5**(12), 909–914 (2009).
20. T. Oo, C. Dong, V. Fiore, and H. Wang, "Evanescently coupled optomechanical system with SiN nanomechanical oscillator and deformed silica microsphere," Appl. Phys. Lett. **103**(3), 031116 (2013).
21. G. Anetsberger, R. Rivière, A. Schliesser, O. Arcizet, and T. J. Kippenberg, "Ultralow-dissipation optomechanical resonators on a chip," Nat. Photonics **2**(10), 627–633 (2008).
22. T. Kato, W. Yoshiki, R. Suzuki, and T. Tanabe, "Octagonal silica toroidal microcavity for controlled optical coupling," Appl. Phys. Lett. **101**(12), 121101 (2012).
23. T. Carmon and K. J. Vahala, "Modal spectroscopy of optoexcited vibrations of a micron-scale on-chip resonator at greater than 1 GHz frequency," Phys. Rev. Lett. **98**(12), 123901 (2007).
24. H. Fan, S. Hua, X. Jiang, and M. Xiao, "Demonstration of an erbium-doped microsphere laser on a silicon chip," Laser Phys. Lett. **10**(10), 105809 (2013).
25. B.-B. Li, Y.-F. Xiao, M.-Y. Yan, W. R. Clements, and Q. Gong, "Low-threshold Raman laser from an on-chip, high-Q, polymer-coated microcavity," Opt. Lett. **38**(11), 1802–1804 (2013).
26. T. Carmon, L. Yang, and K. Vahala, "Dynamical thermal behavior and thermal self-stability of microcavities," Opt. Express **12**(20), 4742–4750 (2004).
27. C. J. Glassbrenner and G. A. Slack, "Thermal conductivity of silicon and germanium from 3 K to the melting point," Phys. Rev. **134**(4A), A1058–A1069 (1964).
28. R. O. Pohl, X. Liu, and E. Thompson, "Low-temperature thermal conductivity and acoustic attenuation in amorphous solids," Rev. Mod. Phys. **74**(4), 991–1013 (2002).
29. D. B. Leviton and B. J. Frey, "Temperature-dependent absolute refractive index measurements of synthetic fused silica," Proc. SPIE **6273**, 62732K (2006).

1. Introduction

Silica whispering gallery mode (WGM) microresonators, such as microtoroids and microspheres, have been used in a variety of photonics applications [1], such as bio/chemical sensors [2–4], low-threshold microlasers [5,6], cavity quantum electrodynamics [7–9], and cavity optomechanics [10–20]. For experimental optomechanical studies, remarkable successes, such as strong coupling in the quantum regime [14], optomechanical light storage [15,16], and coherent optical wavelength conversion via a mechanically-dark optical super mode [17,18] have recently been achieved in these systems. In addition, both microtoroids and microspheres have also been coupled to high-Q nanomechanical oscillators for the development of hybrid optomechanical systems [19,20]. The ultrahigh Q factor and small mode volume of optical WGMs are highly desirable for optomechanical studies. However, the poor thermal conductivity of fused silica, combined with the thin silica layer in a microtoroid or the long fiber stem attached to a microsphere, also leads to laser-heating-induced optical bistability that occurs at extremely low optical power, especially in a vacuum environment, hindering the use of these otherwise excellent optomechanical resonators.

In this paper, we report the fabrication and characterization of chip-based silica microspheres, which are thermally connected to the silicon wafer through a silicon pedestal, thus greatly reducing the threshold optical power for the onset of thermal bistability. We also show that a chip-based silica microsphere can feature mechanical Q factors and optomechanical cooperativity, which are as good as those of a comparable silica microsphere attached to a fiber stem. In addition, the size of the silicon pedestal can be easily controlled through a silicon etching process, which is important for reducing clamping losses [21] induced by the silicon pedestal supporting the silica microsphere. The greatly improved thermal performance should enable the use of these resonators for optomechanical studies in a vacuum environment, which is necessary for overcoming mechanical damping induced by collisions with air molecules, and is also essential for the operation of many cryogenic systems.

2. Fabrication and thermal properties of the chip-based microspheres

Chip-based silica microspheres were fabricated from a silicon wafer with a 3 μm thick silicon dioxide layer. Silica microdisks were initially patterned on the silicon wafer through optical

#246334 Received 20 Jul 2015; revised 7 Sep 2015; accepted 8 Sep 2015; published 8 Oct 2015

lithography, followed by buffered HF wet etching. The subsequent isotropic HNA (HF: HNO_3:CH_3COOH = 1:7:2) wet etching created silicon pedestals underneath the silica microdisks [22]. Finally, the silica disks were vertically irradiated by a focused CO_2 laser pulse with a waist size of 300 μm, an intensity above 100 MW/cm^2, and a duration of 20 ms, melting the silica disks into microspheres under the action of surface tension (see Figs. 1(a) and 1(b)). In order to obtain a high quality spherical structure, the top diameter of the silicon pedestals needs to be less than a tenth of the disk diameter [23–25]. Compared with the traditional XeF_2 dry etching, the HNA wet etching not only undercuts the silica microdisks, but also polishes the silicon pedestals, leading to a much smoother silicon surface than that obtained with the dry etching (see Fig. 1(a)). Note that the selectivity of the HNA etching for silicon and silica is around 5:1, which can be compensated by a mask pattern that features disks with a radius 20% greater than the desired disk radius.

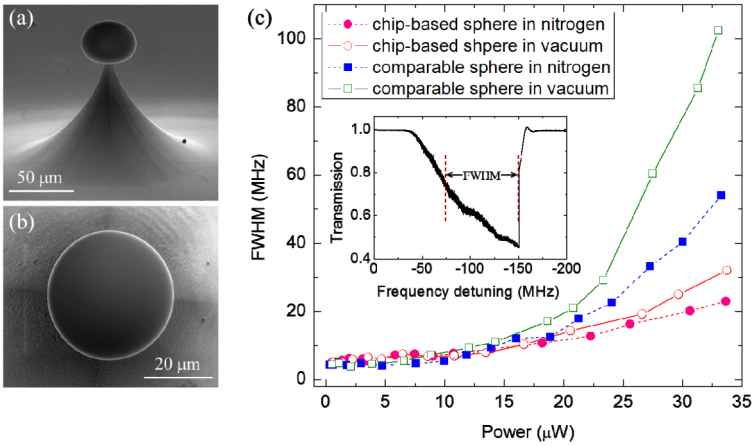

Fig. 1. (a),(b) Side-view and top-view scanning electron micrographs of a silica microsphere on a silicon chip. (c) Full width at half maximum (FWHM) of an optical WGM resonance for a chip-based microsphere and for a comparable microsphere attached to a fiber stem as a function of the input laser power, in either vacuum or nitrogen atmosphere. The inset shows a transmission spectrum, for which the strong asymmetry and the large linewidth broadening are characteristic of laser-heating induced optical bistability.

To characterize the optical and thermal properties of the chip-based microspheres, we excited optical WGMs through a tapere d optical fiber using a probe laser with wavelength near 800 nm. Both the microsphere and the tapered fiber were kept at room temperature in either vacuum or a nitrogen atmosphere in order to prevent contamination from moisture or airborne dust particles. Optical transmission spectra were monitored with an oscilloscope via wavelength scanning. We measured the full width at half maximum (FWHM) of a WGM resonance obtained with a wavelength up-scan as a function of the probe laser power, in either vacuum or nitrogen atmosphere, to determine the threshold power for the onset of laser-heating-induced optical bistability. These results were then compared with those obtained in separate experiments for a comparable traditional silica microsphere attached to a fiber stem (see Fig. 1(c)). Note that the two microspheres feature similar sizes and optical Q factors. The main difference between the two spheres is the pillar or stem material.

At extremely low probe power (< 1 μW), the WGM resonance shows a nearly Lorentzian lineshape and features a loaded Q factor (with a coupling efficiency near 50%) about 7.74 × 10^7 and 8.49 × 10^7 for chip-based and fiber-stem-attached microspheres, respectively. With increasing optical power, the WGM resonance of the fiber-stem-attached microsphere exhibits strong asymmetry and a large linewidth broadening, as shown in the inset of Fig. 1(c). The pronounced triangular-type lineshape shown in the inset in Fig. 1(c) is characteristic of lineshape-broadening and optical bistability induced by laser heating [26].

#246334 Received 20 Jul 2015; revised 7 Sep 2015; accepted 8 Sep 2015; published 8 Oct 2015

In comparison, the chip-based microsphere exhibits much smaller thermal broadening at the same optical power. This robustness against thermal bistability results from the excellent room-temperature thermal conductivity (156 W/(m*K)) of the monocrystalline silicon pedestal [27], which is more than 100 times greater than that of the fused silica (1.38 W/(m*K)) [28]. Note that as shown in Fig. 1(c), both microspheres show much smaller thermal broadening in nitrogen than in vacuum. This is due to the heat conduction of the nitrogen environment.

3. Theoretical calculation of temperature change

To determine the laser-heating-induced temperature change, we assume that the resonance frequency of an optical WGM can be expressed as

$$\omega_0(t) = \frac{\omega_{00}}{1+\alpha\Delta T(t)}. \tag{1}$$

where ω_{00} is the cold cavity resonance frequency and α is the temperature coefficient of WGMs for fused silica, which contains both the thermal expansion and the thermal index change. Near room temperature, $\alpha = 6 \times 10^{-6}$ K^{-1} in the 800 nm wavelength band [29].

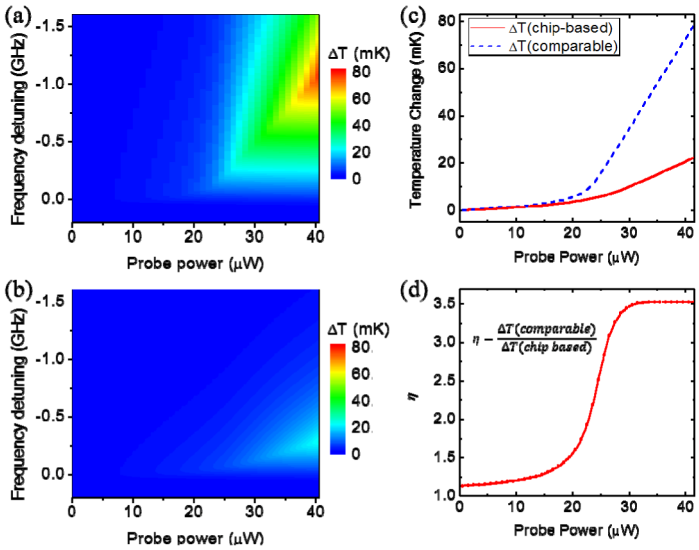

Fig. 2. (a),(b) Temperature changes, derived from experiments, of fiber-attached microsphere (a) and chip-based microsphere (b) in vacuum for different probe powers. (c) Maximum temperature change of the two types of microspheres as a function of the probe power. (d) The ratio (η) of the temperature change between comparable and chip-based sphere as a function of the probe power.

The temperture dynamics of the silica microsphere can be described by [26],

$$C_p\Delta\dot{T}(t) = I\frac{1}{\left(\frac{\Delta\omega(t)}{(\chi_0+\chi_{ex})/2}\right)^2+1} - K\Delta T(t). \tag{2}$$

where C_p is the effective heat capacity (J/K) of the silica microsphere and K is the effective thermal conductivity (W/(m*K)) between silica in the relevant optical mode volume and the rest of the microsphere including the pedestal or stem. I represents the optical power that actually heats the cavity. $\Delta\omega = \omega_p - \omega_0$ is the detuning between the probe laser frequency

#246334 Received 20 Jul 2015; revised 7 Sep 2015; accepted 8 Sep 2015; published 8 Oct 2015

(ω_p) and WGM resonance frequency. χ_0 and χ_{ex} are the intrinsic and external optical energy loss coefficient.

The circulating optical field amplitude evolves according to

$$\dot{a}(t)+[\frac{\chi_0+\chi_{ex}}{2}-i\Delta\omega(t)]a(t)=i\sqrt{\chi_{ex}}s_0. \quad (3)$$

where a and s_0 are respectively the intracavity and the input field amplitude, normalized such that a^2 and s_0^2 correspond to the intracavity photon number and the input photon flux, respectively. With the standard input-output relations for the taper-microcavity system, the amplitude of the output field is given by $s_{out}=s_0+i\sqrt{\chi_{ex}}a(t)$.

By fitting the experimental results of the chip-based and fiber-attached microspheres, we obtained the effective heat capacity and thermal conductivity in vacuum for both microspheres, with K(chip-based) = 2.25 × 10^{-7} W/(m*K), C_p(chip-based) = 6.35 × 10^{-12} J/K, and K(fiber-attached) = 7.44 × 10^{-8} W/(m*K), C_p(fiber-attached) = 6.33 × 10^{-12} J/K. From the theoretical model, we have also derived the induced temperature change (ΔT) of both microspheres as a function of the probe laser frequency and power (see Fig. 2(a) for the fiber-attached microsphere and Fig. 2(b) for the chip-based microsphere). As indicated in Fig. 2, at the same probe laser power the chip-based microsphere exhibits much smaller temperature change than the fiber-attached sphere. The maximum temperature change of both microspheres as well as their ratio, η, at given probe powers can be easily extracted from Figs. 2(a) and 2(b), as plotted in Figs. 2(c) and 2(d), respectively. The slope for the temperature change shown in Figs. 2(c) and 2(d) approaches a constant value when the probe power exceeds 25 μW for the fiber-attached microsphere and 30 μW for chip-based microsphere, respectively. Furthermore, the ratio, η, between maximum temperature changes of the fiber-attached and chip-based microspheres approaches 3.5 when probe laser power exceeds 30 μW. This indicates that compared with the fiber-attached sphere, the more efficient thermal coupling via the silicon pedestal in the chip-based microsphere leads to 3.5 times reduction in the induced laser heating of the silica microsphere.

Furthermore, the monocrystalline silicon has even better thermal conductivity at low temperature (~1500 W/(m*K) at 77 K and ~175 W/(m*K) at 4 K) [27]. In contrast, the thermal conductivity of fused silica decreases drastcially at low temperature (~0.52 W/(m*K) at 77 K and ~0.11 W/(m*K) at 4 K) [28]. In this context, for optical applications such as optomechanical studies, chip-based microspheres can still function well in a cryogenic and vacuum environment, while fiber-attached microspheres are no longer suitable.

4. Mechanical property characterization

We have used the mechanical displacement power spectrum to characterize the mechanical property, and the optomechanically induced transparency (OMIT) to demonstrate the optomechanical coupling for the chip-based microspheres. Figure 3(a) shows a mechanical displacement power spectrum of a radial breathing mode with (n, l) = (1, 2), where n and l are the radial and angular mode numbers of the mechanical mode, respectively. The inset of Fig. 3(a) shows a numerical calculation of the spatial pattern of the breathing mode. The intrinsic mechanical linewidth (γ_m) of this breathing mode is 17.0 kHz, corresponding to a mechanical Q about 5260, which is nearly the same as that of comparable microspheres attached to a fiber stem[16]. Linewidth as narrow as 10 kHz has been observed for the (1, 2) mode.

#246334 Received 20 Jul 2015; revised 7 Sep 2015; accepted 8 Sep 2015; published 8 Oct 2015

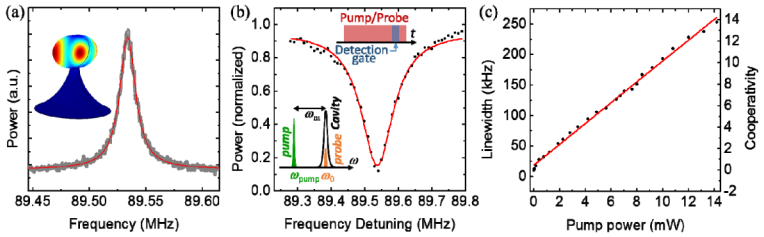

Fig. 3. (a) Mechanical displacement power spectrum of the (1, 2) radial breathing mode of a chip-based microsphere with a diameter of 34 μm. The top diameter of the silicon pedestal is about 6.0 μm. (b) Optomechanically induced transparency (OMIT) spectrum obtained with a pump power of 6.7 mW. Top inset: schematics of the timing for the detection gate and the pump/probe pulse. Bottom inset: Schematics of the spectral position of the pump and probe pulses. (c) Pump power dependence of the measured effective linewidth of the OMIT dip and the corresponding cooperativity.

For the OMIT experiments, pump and probe pulses with the same timing and duration (10 μs) were used. The duty cycle of the experiments was 1%. The pump laser was locked to the red mechanical sideband of a WGM (with linewidth κ = 32 MHz) using a Pound-Drever-Hall technique. The emission power from the cavity mode was measured as a function of the detuning between the fixed pump at the red sideband and a weak and tunable probe near the cavity resonance with a spectrum analyzer (see Fig. 3b), as discussed in detail in earlier experimental studies [15–18]. Note that the spectrum analyzer was operated in a time-gated detection mode, for which the the detection gate with a duration of 1 μs and a resolution bandwidth of 3 MHz was positioned 8 μs from the leading edge of the laser pulses, as shown in the inset of Fig. 3(b). Figure 3(b) shows an example of the OMIT spectrum obtained with an input pump power of about 6.7 mW and when the pump probe detuning is near the frequency of the (1, 2) breathing mode. The optomechanical cooperativity, $C = 4G^2/\kappa\gamma_m$, a dimensionless parameter characterizing the strength of optomechanical coupling, can be derived from the linewidth (FWHM) of the OMIT dip, $\gamma = (1 + C)\gamma_m$ or the depth of the nornalized OMIT dip, $d = \left(C/1+C\right)^2$. For the OMIT spectrum shown in Fig. 3(b), both approaches yield C = 6.9. Figure 3(c) shows the cooperativity derived from the OMIT experiments as a function of the input pump power. At comparable pump power, the cooperativity obtained for the chip-based microsphere is similar to that for a fiber-attached sphere with comparable diameter, mechanical linewidth, and optical linewidth [17]. However, because of the improved thermal performance for the chip-based microsphere, we can achieve greater cooperativity by further increasing the pump laser power. Note that the largest cooperativity shown in Fig. 3(c) is limited by the pump laser power available for the experiment. In comparison, for the fiber-attached microspheres, the cooperativity has been limited to near or below 10 due to laser-heating-induced optical bistability [17].

5. Conclusions

In summary, we have demonstrated that chip-based silica microspheres can feature optical and mechanical properties that are similar to comparable fiber-stem-attached silica microspheres. The thermal coupling through a monocrystalline silicon pedestal greatly improves the thermal performance of the chip-based microspheres, avoiding or minimizing problems such as optical bistability induced by laser heating. Our work opens up avenues for experimental investigations of cavity optomechanics using microsphere-based resonators in vacuum environments.

Acknowledgments

This work is supported by the DARPA-MTO ORCHID program through a grant from AFOSR and by NSF.

#246334 Received 20 Jul 2015; revised 7 Sep 2015; accepted 8 Sep 2015; published 8 Oct 2015